Atmos. Chem. Phys. Discuss., https://doi.org/10.5194/acp-2018-1175
Manuscript under review for journal Atmos. Chem. Phys.
Discussion started: 3 December 2018

Atmospheric Chemistry and Physics Discussions

Differences of the inverted terrestrial ecosystem carbon flux between using GOSAT and OCO-2 XCO_2 retrievals

Hengmao Wang[1], Fei Jiang[1,2*], Jun Wang[1], Weimin Ju[1], Jing M. Chen[1,3]

1 Jiangsu Provincial Key Laboratory of Geographic Information Science and Technology, International Institute for Earth System Science, Nanjing University, Nanjing, 210023, China
2 Jiangsu Center for Collaborative Innovation in Geographical Information Resource Development and Application, Nanjing, 210023, China
3, Department of Geography, University of Toronto, Toronto, Ontario M5S3G3, Canada

Abstract

In this study, both the Greenhouse Gases Observing Satellite (GOSAT) and the Orbiting Carbon Observatory 2 (OCO-2) XCO_2 retrievals are assimilated within the GEOS-Chem 4D-Var assimilation framework to constrain the terrestrial ecosystem carbon flux during Jul 1, 2014 to Dec 31, 2015. The inverted global and regional carbon fluxes during Jan 1 to Dec 31, 2015 are shown and discussed. Surface CO_2 mixing ratios from 47 surface flask sites and XCO_2 measurements from 13 TCCON sites are used to evaluate the simulated concentrations with the posteriori carbon fluxes. The results show that globally, the terrestrial ecosystem carbon sink (excluding biomass burning emissions) estimated from GOSAT data is stronger than that inferred from OCO-2 data, and the annual atmospheric CO_2 growth rate estimated from GOSAT data is more consistent with the estimate of GCP 2017. Regionally, in most regions, the land sinks inferred from GOSAT data are also stronger than those from OCO-2 data. Compared with the prior fluxes, the carbon fluxes in northern temperate regions change most, followed by tropical and southern temperate regions, and the smallest changes occur in boreal regions. Basically, in temperate regions, the inferred land sinks are significantly increased, while those in tropical regions are decreased. The different changes in different regions are mainly related to the spatial coverage and the amount of XCO_2 data in these regions. Compared with CT2016, the inferred carbon sinks are comparable in most temperate regions, but much weaker in

* Corresponding author: Tel.: +86-25-83597077; Fax: +86-25-83592288; E-mail address: jiangf@nju.edu.cn

Atmos. Chem. Phys. Discuss., https://doi.org/10.5194/acp-2018-1175
Manuscript under review for journal Atmos. Chem. Phys.
Discussion started: 3 December 2018

Atmospheric Chemistry and Physics Discussions

boreal and tropical regions. Evaluations using flask and TCCON observations suggest that GOSAT and OCO-2 data, can effectively improve the carbon flux estimates in the northern hemisphere, while in the southern hemisphere the optimized carbon sinks may be overestimated, especially for GOSAT data.

Keywords: Terrestrial ecosystem carbon flux, inversion, GOSAT, OCO-2, GEOS-Chem

1. Introduction

Atmospheric inverse modeling is an effective method for quantifying surface carbon fluxes at global and regional scales using the gradient of CO_2 measurements. Inversion studies based on in-situ CO_2 observations agree well on global carbon budget estimates but differ greatly on regional carbon flux estimates and the partitioning of land and ocean fluxes as well, mainly due to the sparseness of observations in tropics, southern hemisphere oceans and the majority of continental interiors such as those in South America, Africa, and Boreal Asia (Peylin el al., 2013). Satellite observations offer an attractive means to constrain atmospheric inversions with their extensive spatial coverage over remote regions. Studies have shown that satellite observations, though with lower precision than in-situ measurements, can improve the carbon flux estimates (Rayner and O Brien, 2001; Pak and Prather, 2001; Houweling et al., 2004; Baker et al., 2006; Chevallier., 2007; Miller et al., 2007; Kadygrov et al., 2009; Hungershoefer et al., 2010).

Satellite sensors designed specifically to measure atmospheric CO_2 concentrations, have been in operation in recent years. The Greenhouse Gases Observing Satellite (GOSAT) (Kuze et al., 2009), being the first satellite mission dedicated to observing CO_2 from space, was launched in 2009. The National Aeronautics and Space Administration (NASA) launched the Orbiting Carbon Observatory 2 (OCO-2) satellite in 2014 (Crisp et al., 2017; Eldering et al., 2017). China's first CO_2 monitoring satellite (TanSat) was launched in 2016 (Wang et al, 2017; Yang et al, 2017). These satellites measure near-infrared sunlight reflected from the surface in CO_2 spectral bands and the O_2

A-band to retrieve column-averaged dry-air mole fractions of CO_2 (XCO_2), aiming to improving the estimation of spatial and temporal distributions of carbon sinks and sources. A number of inversions have utilized GOSAT XCO_2 retrievals to infer surface carbon fluxes (Takagi et al., 2011; Basu et al., 2013; Maksyutov et al., 2013; Saeki et al., 2013; Chevallier et al., 2014; Deng et al., 2014; Houweling et al., 2015; Deng et al, 2016). Although large uncertainty reductions were achieved for regions which are under-sampled by in-situ observations, these studies didn't give robust regional carbon flux estimates. There are large spreads in regional flux estimates in some regions among these inversions. Furthermore, regional flux distributions inferred from GOSAT XCO_2 data are significantly different from those inferred from in-situ observations. For instance, several studies using GOSAT retrievals reported a larger than expected carbon sink in Europe (Basu et al., 2013; Chevallier et al., 2014; Deng et al., 2014; Houweling et al., 2015). The validity of this large Europe carbon sink derived from GOSAT retrievals is in intense debate and efforts to achieve a consensus estimate of Europe carbon sinks are still ongoing (Reuter et al., 2014; Feng et al., 2016; Reuter et al., 2017).

Compared with GOSAT, OCO-2 has a higher sensitivity near the surface, much finer footprints and more extended spatial coverage, and thus has the potential to better constrain the surface carbon flux inversion (Eldering et al., 2017). Studies have used OCO-2 XCO_2 data to estimate carbon flux anomalies during recent El Nino events (Chatterjee et al., 2017; Patra et al., 2017; Heymann et al., 2017; Liu et al., 2017). Nassar et al. (2017) applied OCO-2 XCO_2 data to infer emissions from large power plants. Miller et al. (2018) evaluated the potential of OCO-2 XCO_2 data in constraining regional biospheric CO_2 fluxes and found that in the current state of development, OCO-2 observations can only provide a reliable constraint on CO_2 budget at continental and hemispheric scales. At present, it is still not clear whether with the improved monitoring capabilities, current OCO-2 observations have a greater potential than GOSAT observations for estimating CO_2 flux at regional or

finer scale. It is therefore important to investigate how current OCO-2 XCO_2 data differ from GOSAT XCO_2 data in constraining carbon budget.

In this study, we evaluate the performance of GOSAT and OCO-2 XCO_2 data in constraining terrestrial ecosystem carbon flux. GOSAT and OCO-2 XCO_2 retrievals produced by the NASA Atmospheric CO_2 Observations from Space (ACOS) team are applied to infer monthly terrestrial ecosystem carbon sinks and sources from Oct, 2014 to December, 2015, using a 4D-Var scheme based on the GEOS-Chem Adjoint model. Inversion results are evaluated against surface flask CO_2 observations and TCCON XCO_2 measurements. We analyze the differences of inverted terrestrial ecosystem carbon flux between using two XCO_2 data. The inverted carbon fluxes are also compared with results from other datasets such as CarbonTracker CT2016 (Peters, et al., 2007) and Global Carbon Project (GCP) 2017 (Le Quéré et al., 2018). This paper is organized as follows. Section 2 briefly introduces GOSAT and OCO-2 XCO_2 retrievals and the inversion methodology and settings. Results and discussions are presented in Section 3, and Conclusions are given in Section 4.

2. Data and Method

2.1 GOSAT and OCO-2 XCO_2 retrievals

Developed jointly by the National Institute for Environmental Studies (NIES), the Japanese Space Agency (JAXA) and the Ministry of the Environment (MOE) of Japan, GOSAT was designed to measure total column abundances of CO_2 and CH_4. The satellite flies at a 666 km altitude in a sun-synchronous orbit with 98° inclination that crosses the equator at 12:49 local time. It covers the whole globe in three days and has a footprint of 10.5 km^2 at nadir. OCO-2 is NASA's first mission dedicated to measuring atmospheric CO_2 concentration. It flies at 705 km altitude in a sun-synchronous orbit with an overpass time at approximately 13:30 local time and a repeat cycle of 16 days. Its grating spectrometer measures reflected sunlight in three near-infrared regions (0.765, 1.61 and 2.06 μm) to retrieve XCO_2. OCO-2 has a footprint of 1.29×2.25 km^2 at nadir and acquires eight

cross-track footprints creating a swath width of 10.3 km.

Both GOSAT and OCO-2 XCO_2 products were created using the same retrieval algorithm, which is based on a Bayesian optimal estimation approach (Roggers et. al., 2000; O Dell et. al., 2011). The GOSAT and OCO-2 XCO_2 data used in this study are Version 7.3 Level 2 Lite products at the pixel level. The XCO_2 data from lite products are bias-corrected (Wunch et. al., 2011). Before used in our inversion system, the data are processed in three steps. First, the retrievals for the glint soundings over oceans have relatively larger uncertainty, thus the data over oceans are not used in our inversions (Wunch et. al., 2017). Second, in order to achieve the most extensive spatial coverage with the assurance of using best quality data available, the XCO_2 data are filtered with two parameters, namely warn_levels and xco2_quality_flag, which are provided along with the XCO_2 data. All data with xco2_quality_flag not equaling 0 are removed, the rest are divided into three groups according the value of warn_levels, namely group 1, group 2 and group 3. In group 1, the warn_levels are less than 8, in group 2, the warn_levels are greater than 9 and less than 12, and in group 3, those are greater than 13. Group 1 has the best data quality, followed by group 2, and group 3 is the worst. Third, the pixel data are averaged within the grid cell of 2°×2.5°, which is the resolution of the global atmospheric transport model used in this study. In each grid of 2°×2.5°, only the groups of best data quality are selected and then averaged. The other variables like column averaging kernel, retrieval error and so on which are provided along with the XCO_2 product are also dealt with the same method. Figures 1a and 1b show the coverages and data amount of GOSAT and OCO-2 XCO_2 data during the study period after processing.

Atmos. Chem. Phys. Discuss., https://doi.org/10.5194/acp-2018-1175
Manuscript under review for journal Atmos. Chem. Phys.
Discussion started: 3 December 2018

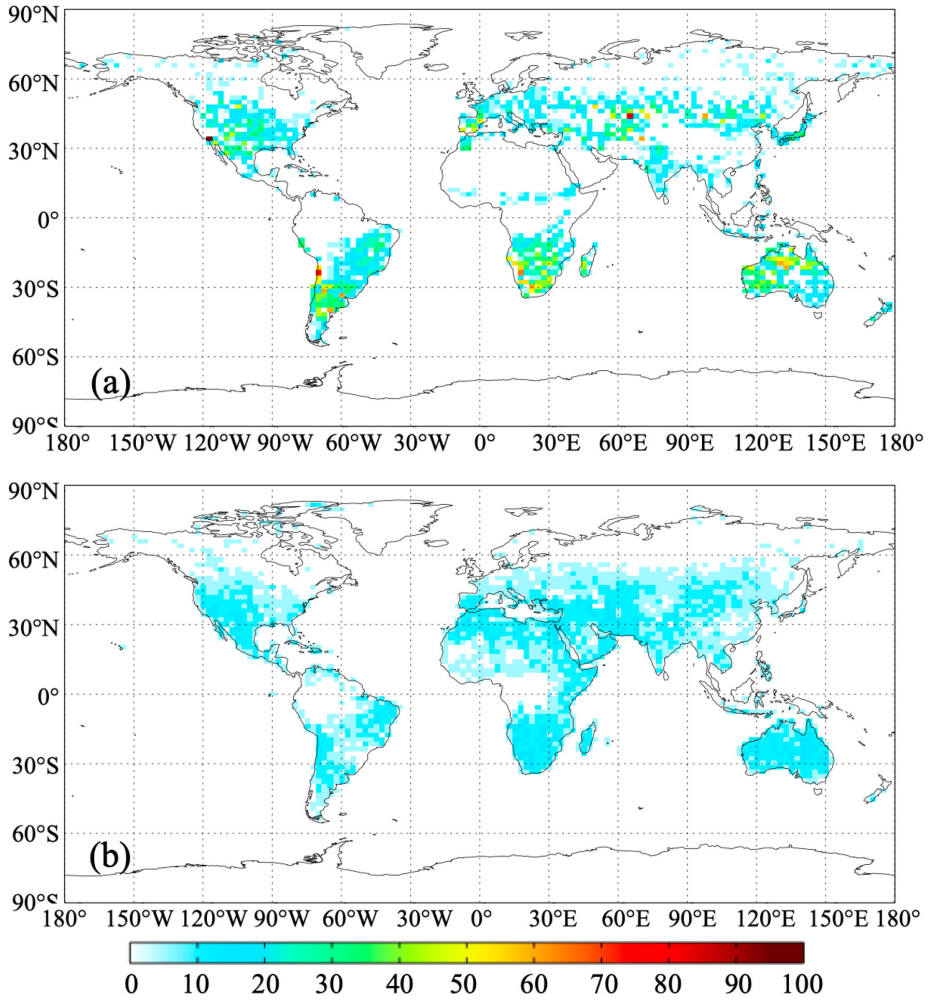

Figure 1. Data amount of each grid cell (2°×2.5°) of ACOS XCO_2 used in this study (a, GOSAT; b, OCO-2)

2.2 Surface flask and TCCON CO_2 measurements

We evaluate the inversion results through comparing the modeled CO_2 mixing ratios using the posteriori fluxes with surface flask measurements and Total Carbon Column Observing Network (TCCON) XCO_2 observations. The flask measurements of CO_2 mixing ratios are downloaded from World Data Center for Greenhouse Gases (WDCGG) under the World Meteorological Organization (WMO) Global Atmospheric Watch (GAW) programme (http://ds.data.jma.go.jp/gmd/wdcgg/). 47

Atmos. Chem. Phys. Discuss., https://doi.org/10.5194/acp-2018-1175
Manuscript under review for journal Atmos. Chem. Phys.
Discussion started: 3 December 2018

Atmospheric Chemistry and Physics Discussions

surface sites which have valid observations for at least two months in 2015 are chosen. TCCON is a network of ground-based Fourier Transform Spectrometers that measure direct near-infrared solar absorption spectra. Column-averaged abundances of atmospheric constituents including CO_2, CH_4, N_2O, HF, CO, H_2O, and HDO are retrieved through these spectra. We use XCO_2 retrievals from 13 stations from TCCON GGG2014 dataset (Blumenstock et al., 2017; Deutscher et al., 2017; Griffith et al., 2017a, b; Kivi et al., 2017; Morino et al., 2017; Notholt et al., 2017a, b; Sherlock et al., 2017; Sussmann and Rettinger, 2017; Warneke et al., 2017; Wennberg et al., 2017a, b). The locations of 47 flask sites and 13 TCCON stations are shown in Figure 2.

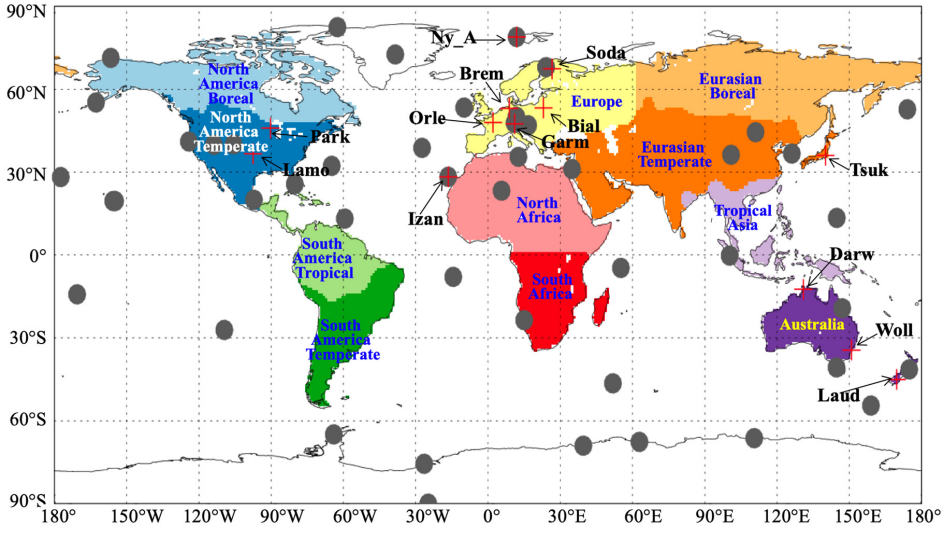

Figure 2. Distributions of the 47 surface flask sites (gray solid circle) and 13 TCCON sites (red cross mark), shaded shows the 11 TRANSCOM regions

2.3 GEOS-Chem 4DVAR assimilation framework

In this work, bias-corrected XCO_2 retrievals are assimilated to estimate monthly terrestrial ecosystem carbon fluxes using the GEOS-Chem and its adjoint model in a 4D-Var assimilation framework.

2.3.1 GEOS-Chem model

GEOS-Chem model (http://geos-chem.org) is a global three-dimensional chemistry transport

model (CTM), which is driven by assimilated meteorological data from the Goddard Earth Observing System (GEOS) of the NASA Global Modeling and Assimilation Office (GMAO) (Rienecker et al., 2008). The original CO_2 simulation in the GEOS-Chem model was developed by Suntharalingam *et al.* (2004) and accounts for CO_2 fluxes from fossil fuel combustion and cement production, biomass burning, terrestrial ecosystem exchange, ocean exchange and biofuel burning. Nassar et al. (2010) updated the CO_2 simulation with improved inventories. In addition to the inventories in earlier version, the new CO_2 fluxes includes CO_2 emissions from international shipping, aviation (3D) and the chemical production of CO_2 from CO oxidation throughout the troposphere. In most other models, the oxidation of CO was treated as direct surface CO_2 emissions. The details of the CO_2 simulation and the CO_2 sinks/sources inventories could be found in Nassar et al. (2010). The version of GEOS-Chem model used in this study is v8-02-01.

2.3.2 GEOS-Chem adjoint model

An adjoint model is used to calculate the gradient of a response function of one model scalar (or cost function) with respect to a set of model parameters. The adjoint of the GEOS-Chem model was first developed for inverse modeling of aerosol (or their precursors) and gas emissions (Henze et al., 2007). It has been implemented to constrain sources of species such as CO, CH_4, and O_3 with satellite observations (Kopacz et al., 2009, 2010; Jiang et al., 2011; Wecht et al., 2012; Parrington et al., 2012). Several studies have successfully used this adjoint model to constraint carbon sources and sinks with surface flask measurements of CO_2 mixing ratio and space-based XCO_2 retrievals (Deng et al., 2014; Liu et al., 2014; Deng et al., 2016; Liu et al., 2017).

2.3.3 Inversion method

In the GEOS-Chem inverse modeling framework, the 4D-Var data assimilation technique is employed for combining observations and simulations to seek a best optimal estimation of the state of a system. This approach seeks the scaling factors of the carbon flux that minimize the cost function, J, given by:

Atmos. Chem. Phys. Discuss., https://doi.org/10.5194/acp-2018-1175
Manuscript under review for journal Atmos. Chem. Phys.
Discussion started: 3 December 2018

Atmospheric Chemistry and Physics Discussions

$$J(\mathrm{c}) = \frac{1}{2}\sum_{i=1}^{N}\left(XCO_{2,i}^{m} - XCO_{2,i}^{obs}\right)S_{obs,i}^{-1}\left(XCO_{2,i}^{m} - XCO_{2,i}^{obs}\right) + \frac{1}{2}(c - c_a)S_c^{-1}(c - c_a) \quad (173)$$

where N is total number of satellite XCO_2 observations; XCO_2^m and XCO_2^{obs} are modeled and observed total column averaged dry air mole faction of CO_2 respectively; c_a is the priori scaling factor of the carbon flux, which is typically set as unity; S_{obs} is the model-data mismatch error covariance matrix; S_c is the scaling factor error covariance matrix. The gradients of the cost function with respect to scaling factors calculated with the adjoint model are supplied to an optimization routine (the L-BFGS-B optimization routine; Byrd et al., 1995; Zhu et al., 1994), and the minimum of the cost function is sought iteratively.

For the modeled CO_2 column to be comparable with the satellite XCO_2 retrievals, the modeled CO_2 concentration profile should be first mapped into the satellite retrieval levels and then convoluted with retrieval averaging kernels. The modeled XCO_2 is computed by:

$$XCO_2^m = XCO_2^a + \sum_j h_j a_j (A(x) - y_{a,j}) \quad (184)$$

where j denotes retrieval level, x is the modeled CO_2 profile; $A(x)$ is a mapping matrix; XCO_2^a is a priori XCO_2, h_j is pressure weighting function, a_j is the satellite column averaging kernel and y_a is the priori CO_2 profile for retrieval.

3. Inversion settings

In this study, the GEOS-Chem model was run in a horizontal resolution of 2°×2.5° for 47 vertical layers. Two experiments, one with GOSAT data and the other with OCO-2 data, were conducted from Oct 1, 2014 to December 31, 2015. The posteriori dry air mole fraction of CO_2 of Oct 1, 2014 from CT2016 product was taken as the initial concentration. The first three months were taken as the spin-up period. The priori carbon fluxes used in this study include: fossil fuel and cement manufacture CO_2 emissions from the Carbon Dioxide Information Analysis Center (CDIAC) (Andres et

al., 2011), biomass burning CO_2 emissions from the Global Fire Emissions Database version 4.1 (GFEDv4) (van der Werf et al., 2010; Giglio et al., 2013) ; terrestrial ecosystem carbon exchanges from the Carnegie-Ames-Stanford Approach (CASA) model GFED4.1 simulation (Potter el al., 1993; van der Werf et al., 2010) ; CO_2 exchanges over the ocean surface from the posteriori air-sea CO_2 flux from CT2016 (Peters *et al.* 2007, with updates documented at http://carbon-tracker.noaa.gov); monthly shipping emissions of CO_2 from the International Comprehensive Ocean–Atmosphere Data Set (ICOADS) (Corbett and Koehler, 2003; Endresen et al., 2004, 2007); 3-D aviation CO_2 emissions (Kim et al., 2007; Wilkerson et al., 2010); and 3-D chemical production of CO_2 from the oxidation of other atmospheric carbon species and its surface corrections (Nassar et al., 2010). It is noted that the terrestrial ecosystem CO_2 exchanges, fossil fuel and cement manufacture emissions and biomass burning emissions in our inversions are the same as those in CT2016. Since we exclude XCO_2 retrievals over ocean, in our inversions, the terrestrial ecosystem exchanges might compensate for the under-constrained ocean CO_2 fluxes. To mitigate the impact of the lack of XCO_2 observations over ocean, we directly use the posteriori ocean CO_2 fluxes of CT2016, which were well constrained with surface flask observations at ocean sites. Only terrestrial ecosystem CO_2 exchanges are optimized in our inversions.

An efficient computational procedure for constructing non-diagonal priori flux error covariance matrix which accounts for the spatial correlation of errors is implemented (Single et al, 2011). The construction is based on the assumption of exponential decay of error correlations. Other than forming covariance matrix explicitly, multiple-dimensional correlations are represented by tensor products of one dimensional correlation matrices along longitude and latitudinal directions. For the two inversions, the scale lengths assigned along longitudinal and latitudinal directions are 500 km and 400 km for terrestrial ecosystem exchange and 1000 km and 800 km for ocean exchange, respectively. No correlations between different types of fluxes are assumed. The temporal correlations are also neglected. Global annual uncertainty of 100% and 40% are assigned for terrestrial ecosystem

Atmos. Chem. Phys. Discuss., https://doi.org/10.5194/acp-2018-1175
Manuscript under review for journal Atmos. Chem. Phys.
Discussion started: 3 December 2018

and ocean CO_2 exchanges, respectively (Deng and Chen, 2011). Accordingly, the ratios of uncertainty to the priori land and ocean fluxes in each month at the grid cell level are assigned with 5 and 3, respectively.

The observation error covariance matrix is constructed using the retrieval error, which is provided along with the XCO_2 data. Observation errors are assumed to be uncorrelated at model grid level. To account for the correlated observation errors, as shown in section 2.1, the pixel level retrieval errors are filtered and averaged to model at the grid level, and then inflated by a factor of 1.9 to ensure the chi-square testing of χ^2 value to be close to 1 (Tarantola, 2004; Chevallier et al., 2007) .

4. Results and Discussions

4.1 Global carbon budget

Table 1 presents the optimized global carbon budgets by the two experiments in 2015. For comparison purposes, the prior fluxes used in this study and the estimates of CT2016 and GCP2017 are also shown in Table 1. The optimized global land sinks based on GOSAT and OCO-2 XCO_2 retrievals are -3.48 and -2.94 PgC yr^{-1}, respectively, which are larger than the prior value, but lower than the CT2016 estimate based on the flask/in-situ CO_2 concentration observations. The differences of ocean fluxes among a priori and two inversions are small since we don't assimilate XCO_2 data over ocean. GCP gives a comprehensive estimate for the global carbon budget every year. In the GCP 2017 estimates, the components of the global carbon budget include fossil fuel and industry, land-use change emissions, atmospheric growth, ocean sink, land sink, and budget imbalance, which are different from those in this study and CT2016 (Table 1). For ease of comparison, the budget imbalance, land sink and land-use change emissions are combined as land net flux, and then the biomass burning emissions and the land sink in this study and those from CT2016 are combined to obtain the land net flux. As shown in Table 1, the prior estimate gives the smallest net land flux (-0.5 Pg C yr^{-1}), and the CT2016 estimate is the largest (-1.7 PgC yr^{-1}). The land net flux optimized based on

Atmos. Chem. Phys. Discuss., https://doi.org/10.5194/acp-2018-1175
Manuscript under review for journal Atmos. Chem. Phys.
Discussion started: 3 December 2018

GOSAT and OCO-2 XCO_2 retrievals fall in between (-0.74 and -1.28 PgC yr^{-1}, respectively), and are much closer to the estimate of GCP 2017 (-1.03 PgC yr^{-1}). A global net flux from GCP is inferred from the global annual atmospheric carbon growth rate, which represents relatively accurately the net carbon flux added into atmosphere. It could be found that the global net flux estimated based on GOSAT data is the closest to the GCP estimate, while the one estimated using OCO-2 data is higher and the CT2016 estimate is much lower than the GCP result, indicating that the land and ocean carbon uptakes in CT2016 were overestimated, while those optimized using OCO-2 data might be underestimated.

Table 1. Global carbon budgets estimated by the OCO-2 experiment, GOSAT experiment in this study as well as those from the priori fluxes, CT2016 and GCP2017 (PgC yr^{-1})

	Priori	OCO-2 experiment	GOSAT experiment	CT2016	GCP2017
Fossil fuel and industry	9.83	9.83	9.83	9.83	9.83
Biomass burning emissions	2.2	2.2	2.2	2.2	1.52[a)]
Land sink	-2.5	-2.94	-3.48	-3.9	-2.55[b)]
Land net flux	-0.5	-0.74	-1.28	-1.7	-1.03
Ocean sink	-2.41	-2.43	-2.45	-2.41	-2.57
Global net flux	7.12	6.66	6.1	5.72	6.23[c)]

[a)] land-use change emissions in GCP2017

[b)] land sink plus budget imbalance

[c)] atmospheric growth

4.2 **Regional carbon flux**

Figure 3 shows the distributions of annual land and ocean carbon fluxes (excluding fossil fuel and biomass burning carbon emissions, same thereafter) of the prior and the estimates using GOSAT and OCO-2 data. It could be found that compared with the prior fluxes, the carbon sinks in Central America, south and northeast China, east and central Europe, south Russia and east Brazil are obviously increased in GOSAT inversion. Except for east Brazil, the land sinks in those areas in OCO-2 inversion are also increased, but much weaker than those in GOSAT inversion, and in east Brazil, it

Atmos. Chem. Phys. Discuss., https://doi.org/10.5194/acp-2018-1175
Manuscript under review for journal Atmos. Chem. Phys.
Discussion started: 3 December 2018

Atmospheric Chemistry and Physics Discussions

turns to a significant carbon source. In contrast, in east and central Canada, north Russia, north Europe, west Indo-China Peninsula, north Democratic Republic of the Congo and west Brazil, their carbon sources are significantly increased in both GOSAT and OCO-2 inversions. In east and central Canada, north Europe and west Brazil, there are much stronger carbon sources in OCO-2 inversion.

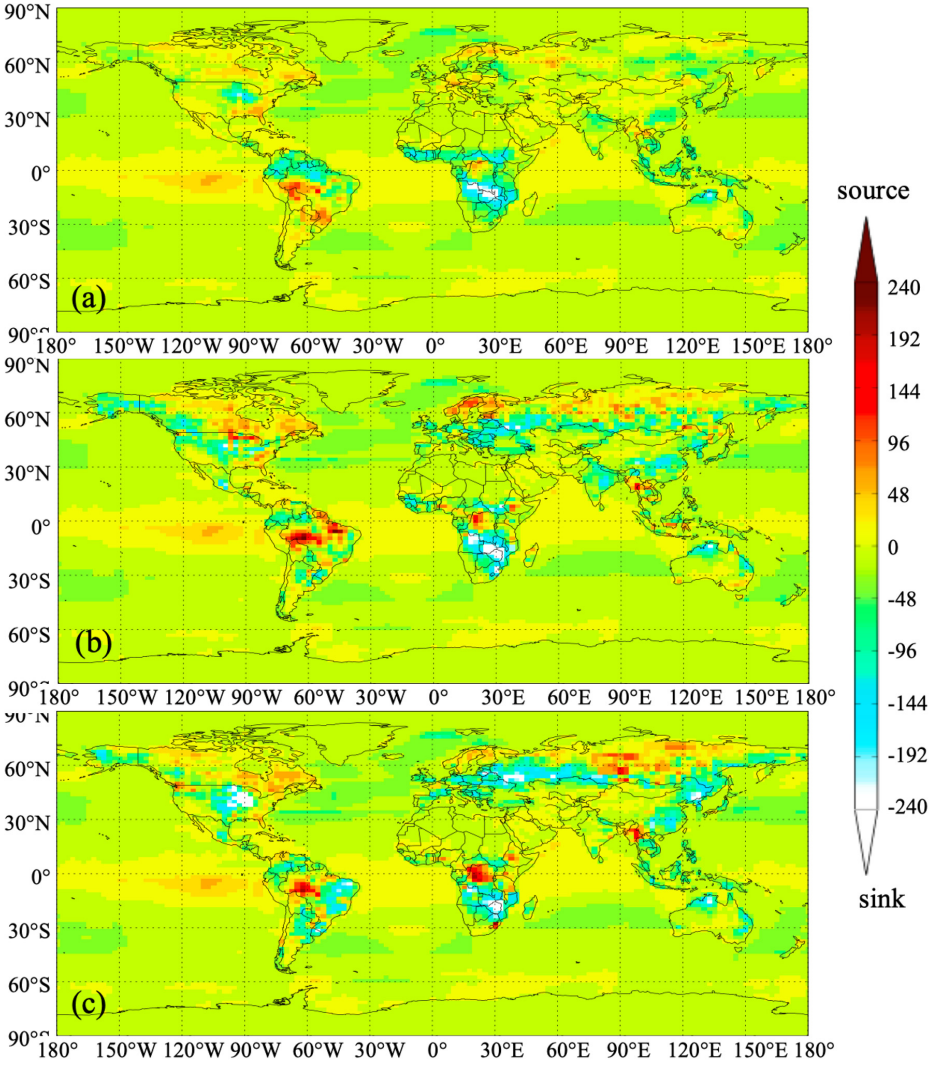

Figure 3. Distributions of annual land and ocean carbon fluxes a) priori flux and posteriori fluxes based on (b) OCO-2 and (c) GOSAT data (gC $m^{-2}yr^{-1}$)

To better investigate the differences between GOSAT and OCO-2 inversions as well as their

Atmos. Chem. Phys. Discuss., https://doi.org/10.5194/acp-2018-1175
Manuscript under review for journal Atmos. Chem. Phys.
Discussion started: 3 December 2018

Atmospheric Chemistry and Physics Discussions

differences with the prior fluxes, we aggregate the prior and inferred land fluxes into 11 TRANSCOM land regions (ref.??). Figure 4 shows aggregated annual land surface fluxes from the prior, GOSAT and OCO-2 inversions for the 11 land regions. For comparison purposes, the optimized surface fluxes in CT2016 are also aggregated and shown in Figure 4.

Clearly, in most regions, the land sinks inverted based on GOSAT data are stronger than those inferred from OCO-2 data. In Northern Temperate and Southern Temperate Lands (i.e., North America Temperate, Eurasian Temperate, Europe, South America Temperate, South Africa and Australia), except for Eurasian Temperate and South Africa, the inferred land sinks using GOSAT XCO_2 are much stronger than those optimized using OCO-2 data. For example, in North America Temperate, the carbon sink of GOSAT experiment (-0.5 Pg C yr^{-1}) is about twice that of the OCO-2 inversions (-0.27 Pg C yr^{-1}); and in South America Temperate, the estimated land sink based on GOSAT data (-0.47 Pg C yr^{-1}) is about 4 times as large as the OCO-2 inversions (-0.12 Pg C yr^{-1}). For the total Temperate Land, the optimized land sinks based on GOSAT and OCO-2 XCO_2 retrievals are -2.95 and -2.59 Pg C yr^{-1}, respectively (Table 2). In the tropics (i.e., South America Tropical, North Africa, and Tropical Asia), except for North Africa, the carbon sinks inferred from GOSAT data are also larger than those estimated using OCO-2 data. In Tropical Asia, the estimated land sink based on GOSAT data (-0.28 Pg C yr^{-1}) is about 2 times of the OCO-2 inversions (-0.13 Pg C yr^{-1}); in South America Tropical, the OCO-2 inversion result is a carbon source of 0.19 PgC yr^{-1}, while GOSAT inversion gives a weak sink of -0.05 Pg C yr^{-1}. The total carbon sinks in tropical land inverted from GOSAT and OCO-2 data are -0.36 and -0.20 Pg C yr^{-1}, respectively. In Northern Boreal Land, including North America Boreal and Eurasian Boreal, the total carbon sinks inverted with GOSAT (-0.18 Pg C yr^{-1}) and OCO-2 (-0.16 Pg C yr^{-1}) data are comparable. However, the two XCO_2 data have opposite performances in these two areas, namely in Eurasian Boreal, the inverted land sink with GOSAT is stronger than that with OCO-2; while in North America Boreal, it is the opposite.

Atmos. Chem. Phys. Discuss., https://doi.org/10.5194/acp-2018-1175
Manuscript under review for journal Atmos. Chem. Phys.
Discussion started: 3 December 2018

Atmospheric Chemistry and Physics Discussions

For different continents (Table 2), in Asia and Australia, their carbon sinks inverted from GOSAT and OCO-2 data are comparable. In North America, South America and Europe, the land sinks in GOSAT inversion are much stronger than those in OCO-2 inversion. Especially in South America, the GOSAT inversion result is a strong carbon sink (-0.51 Pg C yr^{-1}), while in OCO-2 inversion, it is a weak carbon source (0.06 Pg C yr^{-1}). Conversely, in Africa, the land sink estimated with GOSAT data is much weaker than those from OCO-2 data, the former (-0.59 Pg C yr^{-1}) being only about the half of the latter (-1.13 Pg C yr^{-1}).

Compared with the prior fluxes, basically, the inferred land fluxes in Northern Temperate regions have largest changes, followed by those in Tropical regions and Southern Temperate lands, while in boreal regions, the changes are weakest. Basically, in temperate regions, the inferred land sinks are significantly increased, while those in tropical regions are decreased. In boreal regions, the changes using two XCO_2 data are not consistent. As shown in Table 3, in Northern Temperate Land, the increases of carbon sinks constrained by OCO-2 and GOSAT reach to 1.03 and 1.33 Pg C yr^{-1}, respectively, while in Tropical Land, the enhancements of carbon sources are 0.82 and 0.66 Pg C yr^{-1}, respectively, whereas in Northern Boreal Land, the changes caused by the two XCO_2 data are only 0.005 and -0.015 Pg C yr^{-1}. For different TRANSCOM regions and different XCO_2 used, the changes of carbon fluxes have large differences. When using GOSAT data, Europe has the largest change in the carbon flux (-0.63 Pg C yr^{-1}), followed by South America Temperate (-0.50 Pg C yr^{-1}) and North America Temperate (-0.41 Pg C yr^{-1}); when using OCO-2 data, the largest carbon sink changes are in South America Tropical (0.46 Pg C yr^{-1}) and Eurasian Temperate (-0.46 Pg C yr^{-1}), followed by Europe (-0.39 Pg C yr^{-1}). Since the same setup used in these two inversions and the same algorithm adopted for retrieving XCO_2 from GOSAT and OCO-2 measurements, the different impacts of XCO_2 data on land sinks may be related to the spatial coverage and the amount of data in these two XCO_2 datasets. As shown in Figure 1, in different latitude zones, the spatial coverage and the data amount of GOSAT and OCO-2 have large differences. Statistics show that basically, the amount of data is

largest in northern temperate land, followed by southern temperate land and tropical land, and least in northern boreal regions, corresponding to the magnitude of changes of carbon fluxes in these zones. For one specific zone, the different impacts of these two XCO_2 datasets may be also related to their data amount. For example, in northern temperate land, GOSAT has more XCO_2 data than OCO-2. Accordingly, the change of carbon flux caused by GOSAT is larger than that caused by OCO-2. Conversely, in Tropical Land, OCO-2 has more data than GOSAT, and as shown before it has more significant impact on the land sink. This relationship could also be found in each TRANSCOM region. Figure 5 gives a relationship between the XCO_2 data amount ratios of GOSAT to OCO-2 and the land sinks absolute change ratios caused by GOSAT to OCO-2 for 11 TRANSCOM land regions. Obviously, except for North and South Africa, there is a significant linear correlation (R=0.95) between these two ratios, suggesting that the more XCO_2 data, the more carbon flux is changed. In North Africa, we find that OCO-2 has better spatial coverage and more data than GOSAT, as shown in Figure 1, although the differences mainly occur in the Sahara where the carbon flux is very weak, but near the equatorial region where the carbon flux is large, OCO-2 still has more data than GOSAT; in southern Africa, both XCO_2 have good spatial coverage, the amount of GOSAT data is about 1.5 times that of OCO-2, but the changes in the carbon flux caused by GOSAT is about 10 times that of OCO-2. This indicates that in addition to the spatial coverage and the amount of data, the instrument characteristics such as sensor accuracy and spatial resolution may also have impact on the inversion results.

Compared with the CT2016 results, in temperate regions, except for Australia and Europe, the carbon sinks estimated from the two XCO_2 datasets in this study are basically comparable with those inferred based on surface observations in CT2016. In Australia and Europe, the inverted carbon sinks with XCO_2 data in this study are both much stronger than CT2016. Especially in Europe, the CT2016 estimate is a significant source of 0.26 Pg C, whereas our inversions suggest a strong carbon sink ranging between -0.40 and -0.63 Pg C yr^{-1}. Although previous studies (Basu et al., 2013; Chevallier

et al., 2014; Deng et al., 2014; Houweling et al., 2015) also showed enhanced carbon uptake in Europe using GOSAT data, but until now, the strong Europe uptake as inferred from satellite data is still in intense debate (Reuter et al., 2014; Feng et al., 2016; Reuter et al., 2017). Examination of the seasonal variation of the inverted fluxes in Europe shows that during the growing season, both CT2016 and our inversions estimate similar carbon uptake, whereas in the non-growing season, CT2016 produces more carbon release than our inversions. Since there are few satellite measurements in Europe during the dormant season, the carbon release by respiration might not be well constrained by satellite data but close to the prior value.

In boreal regions, the inverted land sinks of CT2016 are significantly stronger than those in this study, especially in the Eurasian Boreal, where the carbon uptake estimated by CT2016 is almost 1 Pg C yr^{-1} larger than our estimates. One explanation for the large sink in CT2016 in this area is that there is a mutual compensation for carbon sinks between Europe and Eurasian Boreal because of the large differences in the amount of observations between these two areas. Kim et al. (2017) found that with the addition of Siberian in-situ measurements to their inversion system, the carbon uptake in Europe was enhanced while it decreased in the boreal Eurasian. Saeki et al. (2013) also reported that more CO_2 observations over Siberian used in the inversion system would weaken the summer carbon uptake in this area. These studies indicate that for CT2016, the carbon sink in Europe may be under-estimated, while in boreal Eurasian, it may be significantly overestimated. Since there are only very few XCO_2 observations from both GOSAT and OCO-2 in this area, our estimates are very close to the prior and much weaker than those found by Saeki et al. (2013) and Kim et al. (2017), indicating that the land sink in the Eurasian Boreal is underestimated in this study. Combined the land sinks of Europe and Eurasian Boreal, the inverted land sinks of GOSAT (-0.86 Pg C yr^{-1}) is comparable with CT2016 (-0.92 Pg C yr^{-1}), indicating that the land sink in Europe inferred from GOSAT may be also overestimated to a certain extent.

In the tropical regions, the inverted land sinks of CT2016 are also all much stronger than our

Atmos. Chem. Phys. Discuss., https://doi.org/10.5194/acp-2018-1175
Manuscript under review for journal Atmos. Chem. Phys.
Discussion started: 3 December 2018

Atmospheric Chemistry and Physics Discussions

373 estimates, but the differences between the inverted and the prior fluxes in CT2016 are significantly
374 smaller than those in this study, mainly because of the lack of surface CO_2 observations in tropical
375 areas, especially in Tropical Asia.

376 For different continents (Table 2), the largest difference between this study and CT2016 is found
377 in Asia. Using an ensemble of seven atmospheric inverse systems, Thompson et al. (2016) reported
378 that the Asian land biosphere CO_2 flux (including land-use change and fires) was a net sink of −0.46
379 (−0.70~0.24) Pg C yr^{-1} (median and range) for 1996–2012. The land biosphere CO_2 fluxes (also in-
380 cluding biomass burning emissions) estimated based on OCO-2 and GOSAT in this study are -0.37
381 and -0.42 Pg C yr^{-1}, respectively, which are comparable with the result of Thompson et al. (2016).
382

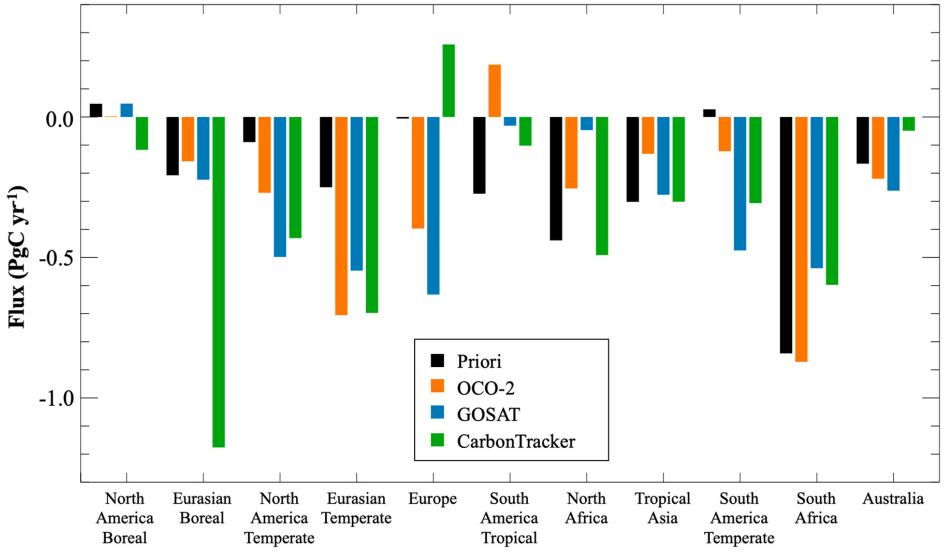

383

384 **Figure 4**. Aggregated annual land fluxes of the 11 TRANSCOM land regions

385
386
387
388

Atmos. Chem. Phys. Discuss., https://doi.org/10.5194/acp-2018-1175
Manuscript under review for journal Atmos. Chem. Phys.
Discussion started: 3 December 2018

Atmospheric Chemistry and Physics Discussions

389 **Table 2**. The priori and posteriori fluxes in six continents and boreal, temperate and tropical lands

Regions	Prior	OCO-2	GOSAT	CT2016
North America	-0.04	-0.27	-0.45	-0.55
South America	-0.25	0.06	-0.51	-0.41
Europe	-0.01	-0.40	-0.63	0.26
Asia	-0.76	-0.99	-1.05	-2.18
Africa	-1.28	-1.13	-0.59	-1.09
Australia	-0.17	-0.22	-0.26	-0.05
Northern Boreal Land	-0.16	-0.16	-0.18	-1.29
Northern Temperate Land	-0.35	-1.37	-1.68	-0.87
Tropical Land	-1.01	-0.20	-0.36	-0.90
Southern Temperate Land	-0.98	-1.21	-1.28	-0.95

390

391 **Table 3**. Differences between the inferred and the prior carbon fluxes, and the data amount of XCO_2
392 in different regions

Region	**Differences (Pg C yr^{-1})**		**XCO_2 data amount**	
	OCO-2	**GOSAT**	**OCO-2**	**GOSAT**
North America Boreal	-0.05	0.00	1143	639
North America Temperate	-0.18	-0.41	2390	3163
South America Tropical	0.46	0.24	800	421
South America Temperate	-0.15	-0.50	1711	3500
North Africa	0.19	0.39	3208	674
South Africa	-0.03	0.30	2057	3060
Eurasian Boreal	0.05	-0.02	1714	1339
Eurasian Temperate	-0.46	-0.30	5323	4782
Tropical Asia	0.17	0.03	726	550
Australia	-0.05	-0.10	2011	3110
Europe	-0.39	-0.63	1604	2106
Global land	-0.44	-0.98	22687	23344
Northern Boreal Land	0.005	-0.02	2857	1978
Northern Temperate Land	-1.03	-1.33	9317	10051
Tropical Land	0.82	0.66	4734	1645
Southern Temperate Land	-0.23	-0.30	5779	9670

Atmos. Chem. Phys. Discuss., https://doi.org/10.5194/acp-2018-1175
Manuscript under review for journal Atmos. Chem. Phys.
Discussion started: 3 December 2018

Atmospheric Chemistry and Physics Discussions

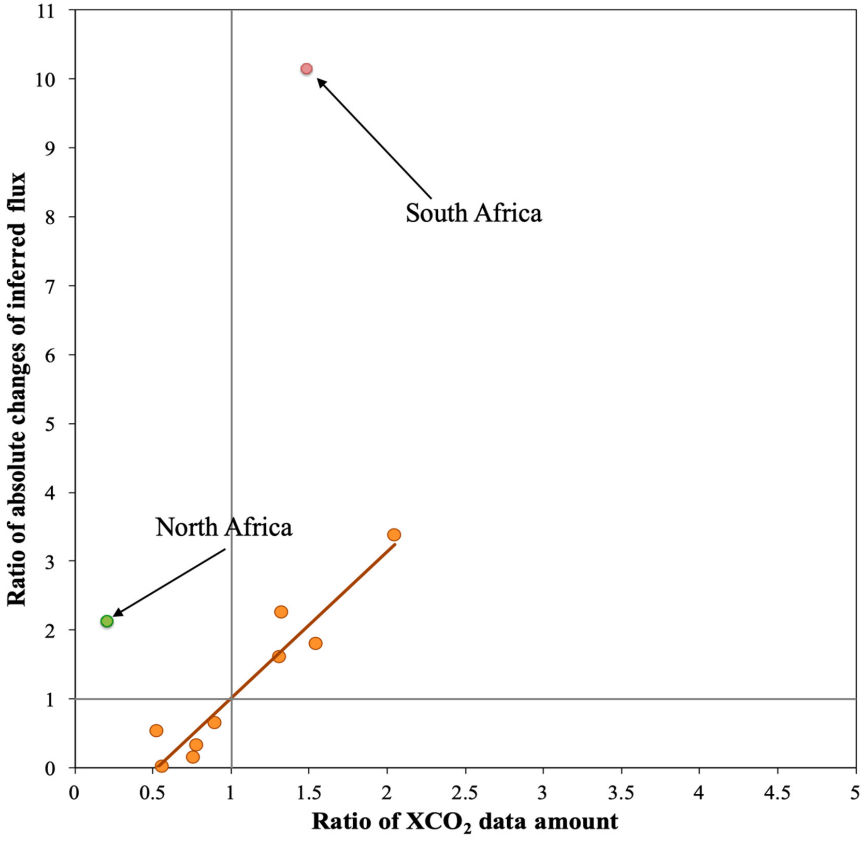

Figure 5. Scatter plot for the ratio of GOSAT to OCO-2 XCO_2 data amount versus the ratio of absolute changes of the land sinks caused by GOSAT to OCO-2 in the 11 TRANSCOM land regions

4.3 Evaluation for the inversion results

4.3.1 Flask observations

We use flask observations from 47 surface sites (Figure 2) to evaluate the posterior fluxes. The GEOS-Chem model is driven with the prior flux and the two posterior fluxes to obtain the prior and posterior CO_2 mixing ratios. The simulated CO_2 mixing ratios are sampled at each observation site and within half an hour of observation time. Figure 6 shows a summary of comparisons of the simulated CO_2 mixing ratio against the flask measurements. The mean difference between the prior CO_2 mixing ratio and the flask measurements is 1.14 ppm, with a standard deviation of 2.73 ppm. Using

406 posterior fluxes inferred from GOSAT and OCO-2 data, the mean differences between the posterior
407 CO_2 mixing ratio and flask measurements are reduced to -0.32 and 0.48 ppm, with a standard devia-
408 tion of 2.59 and 2.79 ppm, respectively. It is noted that the mean difference in the posterior CO_2
409 mixing ratio between GOSAT and OCO-2 inversions at 47 observation sites is 0.8 ppm, much larger
410 than the 0.26 ppm (0.56 Pg C/2.12 Pg C/ppm=0.26 ppm) difference between their global net flux
411 estimates, indicating the relatively large difference in posterior flux between these two inversions at
412 the regional scale. Figure 7 shows the biases at each observation site in different latitudes. It could be
413 found that the biases between the simulations and the observations in the northern hemisphere are
414 significantly larger than those in southern hemisphere since the carbon flux distribution of the north-
415 ern hemisphere is more complex than that of the southern hemisphere. When the prior flux is used,
416 almost all sites in the northern hemisphere have significant positive deviations, with an average of
417 1.7 ppm, while in the southern hemisphere, the deviations are very small, with an average bias of
418 only 0.08 ppm; when using the posteriori flux of OCO-2, the deviations in most northern hemisphere
419 sites are significantly reduced, with the average deviation falling to half the original, to 0.85 ppm,
420 while in the southern hemisphere, at most sites, the biases increase by variable amounts, with a mean
421 of -0.13 ppm; when using the posterior flux of GOSAT, the deviations are further reduced to -0.04
422 ppm in the northern hemisphere but further increased to -0.55 ppm in the southern hemisphere. These
423 suggest that GOSAT and OCO-2 data can effectively improve the carbon fluxes estimate in the north-
424 ern hemisphere, but overestimate the land sinks in the southern hemisphere, especially for GOSAT.
425

Atmos. Chem. Phys. Discuss., https://doi.org/10.5194/acp-2018-1175
Manuscript under review for journal Atmos. Chem. Phys.
Discussion started: 3 December 2018

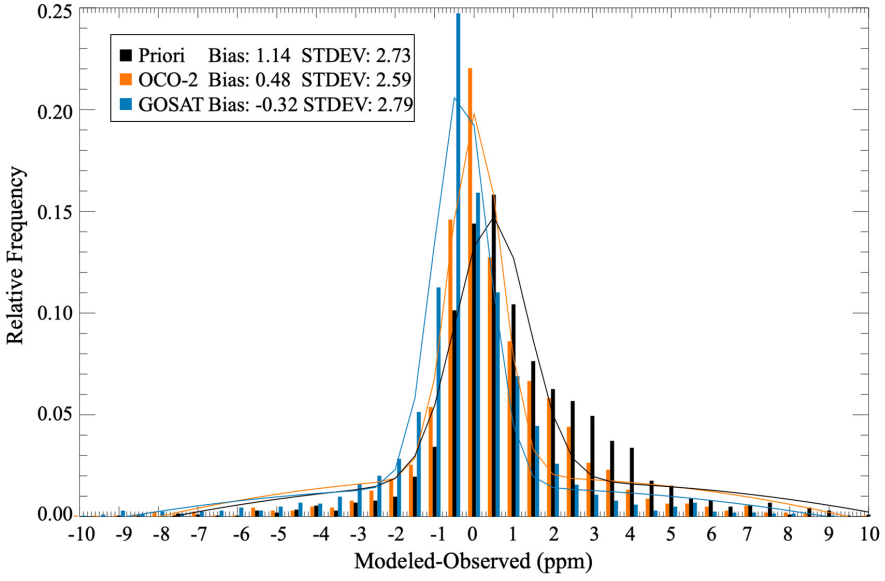

Figure 6. Statistical distribution of the modeled and observed mismatch errors in 47 surface flask sites

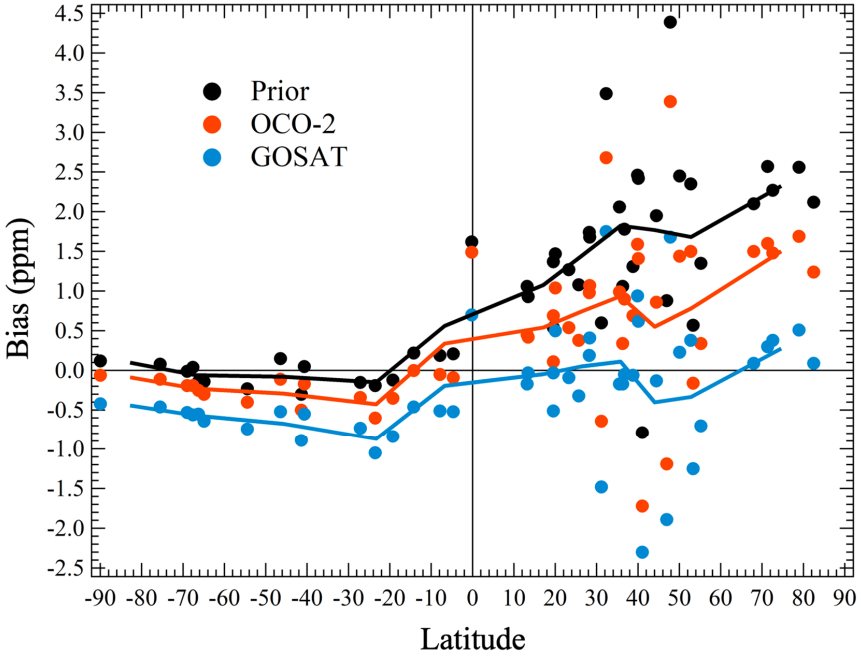

Figure 7. Biases of the simulated CO_2 mixing ratios against the flask measurements in different latitudes (positive/negative biases represent modeled concentration being greater/less than the observed)

Atmos. Chem. Phys. Discuss., https://doi.org/10.5194/acp-2018-1175
Manuscript under review for journal Atmos. Chem. Phys.
Discussion started: 3 December 2018

433 **4.3.2 TCCON observations**

434 We also use ground XCO_2 observations from 13 TCCON sites (Figure 2) to evaluate our inver-
435 sion results. The simulated CO_2 concentrations at 47 vertical levels are mapped into 71 TCCON
436 levels. Following the approach of Wunch et al. (2011), using prior profiles and the averaging kernel
437 from the TCCON dataset, we calculated the modeled XCO_2 values at 13 TCCON sites. Figure 6
438 shows the comparison of modeled XCO_2 with TCCON observations. The mean difference between
439 prior XCO_2 and TCCON observations is 1.37 ppm, with a standard deviation of 1.25 ppm. Through
440 OCO-2 inversion, the mean difference between modeled and observed XCO_2 is slightly reduced to
441 0.93 ppm, with a standard deviation of 1.07 ppm, and through GOSAT inversion, the mean differ-
442 ence between modeled and observed XCO_2 is significantly reduced to 0.04 ppm with a standard de-
443 viation of 1.09 ppm. Figure 9 shows the bias at each TCCON site. Obviously, the biases at all
444 TCCON sites are positive when using the prior fluxes, ranging between 0.3 and 2.6 ppm. The bi-
445 ases at the sites in the northern temperate and boreal areas are all above 1.5 ppm except for the La-
446 mont site. After using the posterior fluxes of OCO-2, the biases of all sites are reduced by 30%. Af-
447 ter using the posteriori fluxes of GOSAT, the biases are significantly reduced, ranging between -
448 0.48 and 1.03 ppm. For two of the three TCCON sites in the southern hemisphere, the biases are
449 changed to negative values when using the posteriori fluxes from GOSAT data, further indicating
450 the overestimation of carbon sinks by GOSAT data in the southern hemisphere.

Atmos. Chem. Phys. Discuss., https://doi.org/10.5194/acp-2018-1175
Manuscript under review for journal Atmos. Chem. Phys.
Discussion started: 3 December 2018

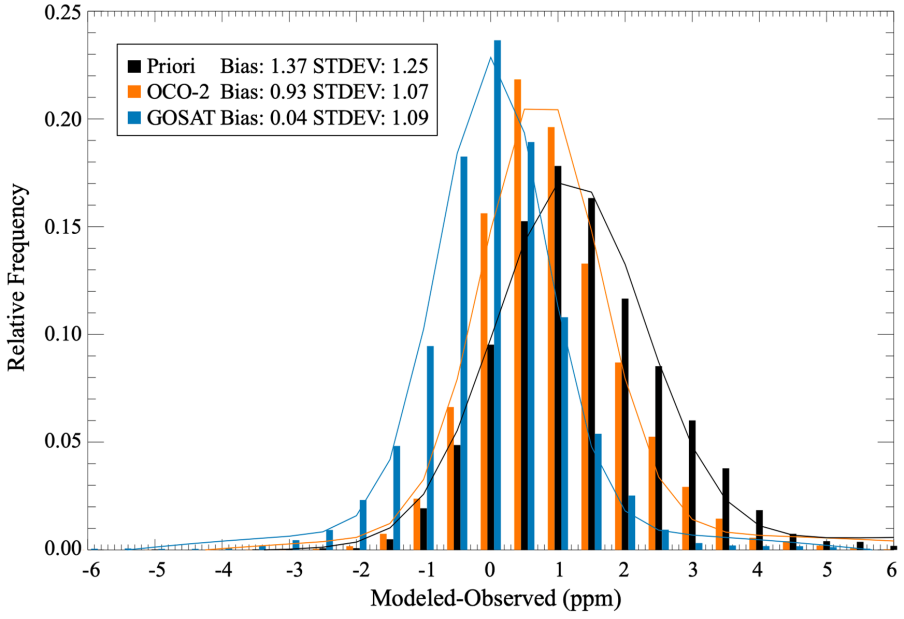

Figure 8. Statistical distributions of modeled and observed mismatch errors at 13 TCCON sites

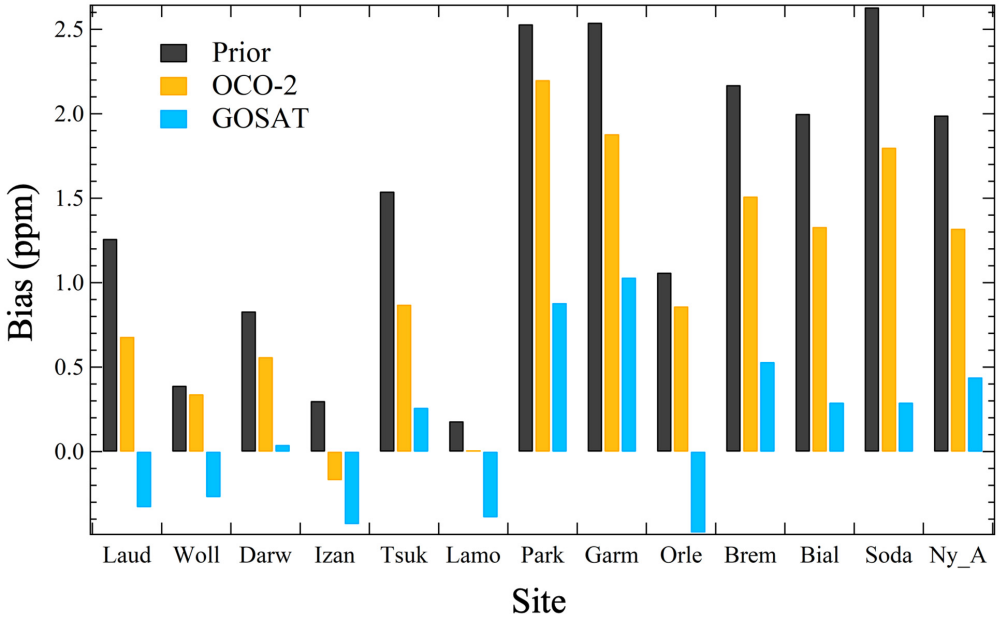

Figure 9. The biases between the modeled and observed XCO_2 at the 13 TCCON sites

Atmos. Chem. Phys. Discuss., https://doi.org/10.5194/acp-2018-1175
Manuscript under review for journal Atmos. Chem. Phys.
Discussion started: 3 December 2018

5. Summary and Conclusions

In this study, we use both GOSAT and OCO-2 XCO_2 retrievals to constrain terrestrial ecosystem carbon fluxes from Oct 1, 2014 to Dec 31, 2015, using a 4D-Var system within the GEOS-Chem adjoint model. The posterior carbon fluxes estimated from GOSAT and OCO-2 data at both global and regional scales during Jan 1 to Dec 31, 2015 are shown and discussed. Surface CO_2 mixing ratios from 47 surface flask sites and XCO_2 observations from 13 TCCON sites are used to evaluate the inversions of carbon fluxes using GOSAT and OCO-2 data.

Globally, the land net flux (including fossil fuel and biomass burning emissions) inferred from GOSAT and OCO-2 XCO_2 retrievals are larger than the prior value, and lower than the estimate of CT2016, but much closer to the estimate of GCP 2017. The terrestrial ecosystem carbon sink (excluding biomass burning emissions) estimated from GOSAT data is stronger than that inferred from OCO-2 data, and the annual atmospheric CO_2 growth rate (global net flux) estimated based on GOSAT data is more consistent with the GCP estimate than that based on OCO-2. Regionally, in most regions, the land sinks inverted based on GOSAT data are also stronger than those inferred from OCO-2 data. Compared with the prior fluxes, basically, the inferred land sinks are significantly increased in northern and southern temperate regions, and decreased in tropical regions. In addition, the inferred carbon fluxes have the largest changes in Northern Temperate regions, followed by Tropical and Southern Temperate regions, and the weakest in boreal regions. The different impact of XCO_2 on the carbon fluxes in different regions are mainly related to the spatial coverage and the amount of XCO_2 data. Generally, a larger amount of XCO_2 data in a region is corresponding to a larger change in the inverted carbon flux in the same region. Compared with the CT2016 results, the carbon sinks optimized using XCO_2 in this study are comparable with CT2016 in most temperate regions, but much weaker than CT2016 in the boreal and tropical regions.

Evaluations of the inversions using CO_2 concentrations from flask and TCCON measurements showed that both posterior carbon fluxes of OCO-2 and GOSAT could significantly improve the

481 modeling of atmospheric CO_2 concentrations, and both the simulated surface CO_2 mixing ratio and
482 XCO_2 concentrations with GOSAT posterior fluxes are much closer to the observations than those
483 with OCO-2. Generally, in the northern hemisphere, the deviations are significantly reduced, while
484 in the southern hemisphere, the biases are elevated to a certain extent. These suggest that GOSAT and
485 OCO-2 data can effectively improve the carbon fluxes estimate in the northern hemisphere, while in
486 the southern hemisphere and some northern temperate regions, the optimized carbon sinks may be
487 overestimated.

488 **Author contributions**

489 FJ and HW designed the research, HW conducted inverse modeling, HW and FJ conducted data anal-
490 ysis and wrote the paper, JW, WJ and JC participated in the discussion of the results and provided
491 input on the paper for revision before submission.

492 **Competing interests**

493 The authors declare that they have no conflict of interest.

494 **Acknowledgements**

495 This work is supported by the National Key R&D Program of China (Grant No: 2016YFA0600204), National
496 Natural Science Foundation of China (Grant No: 41571452), and the Fundamental Research Funds for the
497 Central Universities (Grant No: 090414380021).

498

499 **References**

500 Andres, R. J., Gregg, J. S., Losey, L., Marland, G. and Boden, T. A.: Monthly, global emissions of carbon
501 dioxide from fossil fuel consumption. Tellus B, 63(3), 309–327, https://doi.org/10.1111/j.1600-
502 0889.2011.00530.x, 2011.

503 Baker, D. F., Bösch, H., Doney, S. C., O'Brien, D., and Schimel, D. S.: Carbon source/sink information pro-
504 vided by column CO_2 measurements from the Orbiting Carbon Observatory, Atmos. Chem. Phys., 10,
505 4145–4165, https://doi.org/10.5194/acp-10- 4145-2010, 2010.

506 Basu, S., Guerlet, S., Butz, A., Houweling, S., Hasekamp, O., Aben, I., Krummel, P., Steele, P., Langenfelds,
507 R., Torn, M., Biraud, S., Stephens, B., Andrews, A., and Worthy, D.: Global CO_2 fluxes estimated from
508 GOSAT retrievals of total column CO_2, At- mos. Chem. Phys., 13, 8695–8717,
509 https://doi.org/10.5194/acp- 13-8695-2013, 2013.

510 Basu, S., Krol, M., Butz, A., Clerbaux, C., Sawa, Y., Machida, T., Matsueda, H., Frankenberg, C., Hasekamp,
511 O. P., and Aben, I.: The seasonal variation of the CO_2 flux over Tropical Asia estimated from GOSAT,
512 CONTRAIL, and IASI, Geophys. Res. Lett., 41, 1809–1815, https://doi.org/10.1002/2013GL059105,
513 2014.

514 Blumenstock, T., Hase, F., Schneider, M., García, O.E., and Sepúlveda, E.: TCCON data from Izana, Tene-
515 rife, Spain, Release GGG2014R1. TCCON data archive, hosted by CaltechDATA, California Institute of
516 Technology, Pasadena, CA, U.S.A. https://doi.org/10.14291/tccon.ggg2014.izana01.R1, 2017.

517 Byrd, R. H., Nocedal, J. and Schnabel, R. B.: Representations of Quasi-Newton Matrices and their use in
518 Limited Memory Methods. Math Program. 63(4), 129–156. https://doi.org/10.1007/BF01582063, 1994.

519 Chatterjee, A., Gierach, M. M., Sutton, A. J., Feely, R. A., Crisp, D., Eldering, A., Gunson, M. R., O'Dell, C.
520 W., Stephens, B. B., and Schimel, D. S.: Influence of El Niño on atmospheric CO_2 over the tropical Pa-
521 cific Ocean: Find- ings from NASA's OCO-2 mission, Science, 358, eaam5776,
522 https://doi.org/10.1126/science.aam5776, 2017.

523 Chevallier, F., Bron, F.-M., and Rayner, P. J.: Contribution of the Orbiting Carbon Observatory to the estima-
524 tion of CO_2 sources and sinks: Theoretical study in a variational data assimilation framework, J. Geophys.
525 Res.-Atmos., 112, d09307, https://doi.org/10.1029/2006JD007375, 2007.

526 Chevallier, F., Feng, L., Bösch, H., Palmer, P. I., and Rayner, P. J.: On the impact of transport model errors
527 for the estimation of CO_2 surface fluxes from GOSAT observations, Geophys. Res. Lett., 37, L21803,
528 https://doi.org/10.1029/2010GL044652, 2010.

529 Chevallier, F., Palmer, P. I., Feng, L., Boesch, H., O'Dell, C. W., and Bousquet, P.: Toward robust and con-
530 sistent regional CO_2 flux estimates from in situ and spaceborne measurements of atmospheric CO_2, Ge-
531 ophys. Res. Lett., 41, 1065–1070, https://doi.org/10.1002/2013GL058772, 2014.

532 Corbett, J. J., and Koehler, H. W.: Updated emissions from ocean shipping, J. Geophys. Res., 108, 4650,
533 https://doi.org/10.1029/2003JD003751, D20, 2003.

534 Conway, T. J., Tans, P. P., Waterman, L. S., Thoning, K. W., Kitzis, D. R., Masarie, K. A., and Zhang, N.: Ev-
535 idence for interannual variability of the carbon cycle from the National Oceanic and Atmospheric Admin-
536 istration/Climate Monitoring and Diagnostics Laboratory Global Air Sampling Network, J. Geophys.
537 Res., 99, 22831–22855, https://doi.org/10.1029/94JD01951, 1994.

538 Crisp, D., Pollock, H. R., Rosenberg, R., Chapsky, L., Lee, R. A. M., Oyafuso, F. A., Frankenberg, C.,
539 O'Dell, C. W., Bruegge, C. J., Doran, G. B., Eldering, A., Fisher, B. M., Fu, D., Gunson, M. R., Man-
540 drake, L., Osterman, G. B., Schwandner, F. M., Sun, K., Taylor, T. E., Wennberg, P. O., and Wunch, D.:
541 The on-orbit performance of the Orbiting Carbon Observatory-2 (OCO-2) instrument and its radiometri-
542 cally calibrated products, Atmos. Meas. Tech., 10, 59–81, https://doi.org/10.5194/amt-10-59-2017, 2017.

543 Deng, F. and Chen, J. M.: Recent global CO_2 flux inferred from atmospheric CO_2 observations and its re-
544 gional analyses, Biogeo- sciences, 8, 3263–3281, https://doi.org/10.5194/bg-8-3263-2011, 2011.

545 Deng, F., Jones, D. B. A., Henze, D. K., Bousserez, N., Bowman, K. W., Fisher, J. B., Nassar, R., O'Dell, C.,
546 Wunch, D., Wennberg, P. O., Kort, E. A., Wofsy, S. C., Blumenstock, T., Deutscher, N. M., Griffith, D. W.
547 T., Hase, F., Heikkinen, P., Sherlock, V., Strong, K., Sussmann, R., and Warneke, T.: Inferring regional
548 sources and sinks of atmospheric CO_2 from GOSAT XCO_2 data, Atmos. Chem. Phys., 14, 3703-3727,
549 https://doi.org/10.5194/acp-14-3703-2014, 2014.

550 Deng, F., Jones, D. B. A., O'Dell, C. W., Nassar, R., and Parazoo, N. C.: Combining GOSAT XCO_2 observa-
551 tions over land and ocean to improve regional CO_2 flux estimates, J. Geophys. Res. Atmos., 121, 1896–
552 1913, https://doi.org/10.1002/2015JD024157, 2016.

553 Deutscher, N., Notholt, J., Messerschmidt, J., Weinzierl, C., Warneke, T., Petri, C., Grupe, P., and Katrynski,
554 K.: TCCON data from Bialystok, Poland, Release GGG2014R1. TCCON data archive, hosted by Cal-
555 techDATA, California Institute of Technology, Pasadena, CA, U.S.A.
556 http://doi.org/10.14291/tccon.ggg2014.bialystok01.R1/1183984, 2017.

557 Eldering, A., Boland, S., Solish, B., Crisp, D., Kahn, P., and Gunson, M.: High precision atmospheric CO_2

measurements from space: The design and implementation of OCO-2, in: 2012 IEEE Aerospace Conference, 1–10, https://doi.org/10.1109/AERO.2012.6187176, 2012.

Eldering, A., O'Dell, C. W., Wennberg, P. O., Crisp, D., Gunson, M. R., Viatte, C., Avis, C., Braverman, A., Castano, R., Chang, A., Chapsky, L., Cheng, C., Connor, B., Dang, L., Doran, G., Fisher, B., Frankenberg, C., Fu, D., Granat, R., Hobbs, J., Lee, R. A. M., Mandrake, L., McDuffie, J., Miller, C. E., Myers, V., Natraj, V., O'Brien, D., Osterman, G. B., Oyafuso, F., Payne, V. H., Pol- lock, H. R., Polonsky, I., Roehl, C. M., Rosenberg, R., Schwand- ner, F., Smyth, M., Tang, V., Taylor, T. E., To, C., Wunch, D., and Yoshimizu, J.: The Orbiting Carbon Observatory-2: first 18 months of science data products, Atmos. Meas. Tech., 10, 549–563, https://doi.org/10.5194/amt-10-549-2017, 2017a.

Eldering, A., Wennberg, P. O., Crisp, D., Schimel, D. S., Gun- son, M. R., Chatterjee, A., Liu, J., Schwandner, F. M., Sun, Y., O'Dell, C. W., Frankenberg, C., Taylor, T., Fisher, B., Oster- man, G. B., Wunch, D., Hakkarainen, J., Tamminen, J., and Weir, B.: The Orbiting Carbon Observatory-2 early science investigations of regional carbon dioxide fluxes, Science, 358, eaam5745, https://doi.org/10.1126/science.aam5745, 2017b.

Endresen, Ø., Sørgård, E., Behrens, H. L., Brett, P. O., and Isaksen, I. S. A.: A historical reconstruction of ships' fuel consumption and emissions, J. Geophys. Res., 112, D12301, https://doi.org/10.1029/2006JD007630, 2007.

Feng, L., Palmer, P. I., Parker, R. J., Deutscher, N. M., Feist, D. G., Kivi, R., Morino, I., and Sussmann, R.: Estimates of European uptake of CO_2 inferred from GOSAT XCO_2 retrievals: Sensitivity to measurement bias inside and outside Europe. Atmos. Chem. Phys., 16, 1289–1302, https://doi.org/10.5194/acp-16-1289-2016, 2016.

Giglio, L., Randerson, J. T., and van der Werf, G. R.: Analysis of daily, monthly, and annual burned area using the fourth-generation global fire emissions database (GFED4) J. Geophys. Res. Biogeosci., 118, 317–328, https://doi.org/10.1002/jgrg.20042, 2013.

Griffith, D. W. T., Deutscher, N., Velazco, V. A., Wennberg, P. O., Yavin, Y., Keppel Aleks, G., Washenfelder, R., Toon, G. C., Blavier, J.-F., Murphy, C., Jones, N., Kettlewell, G., Connor, B., Macatangay, R., Roehl, C., Ryczek, M., Glowacki, J., Culgan, T., and Bryant, G.: TCCON data from Darwin, Australia, Release GGG2014R0. TCCON data archive, hosted by CaltechDATA, California Institute of Technology, Pasadena, CA, U.S.A. http://doi.org/10.14291/tccon.ggg2014.darwin01.R0/1149290, 2017a.

Griffith, D. W. T., Velazco, V. A., Deutscher, N., Murphy, C., Jones, N., Wilson, S., Macatangay, R., Kettlewell, G., Buchholz, R. R., and Riggenbach, M.: TCCON data from Wollongong, Australia, Release GGG2014R0. TCCON data archive, hosted by CaltechDATA, California Institute of Technology, Pasadena, CA, U.S.A. https://doi.org/10.14291/tccon.ggg2014.wollongong01.R0/1149291, 2017b.

Henze, D. K., Hakami, A. and Seinfeld, J. H.: Development of the adjoint of GEOS-Chem, Atmos. Chem. Phys., 7, 2413-2433, 2007.

Heymann, J., Reuter, M., Buchwitz, M., Schneising, O., Bovens- mann, H., Burrows, J. P., Massart, S., Kaiser, J. W., and Crisp, D.: CO_2 emission of Indonesian fires in 2015 estimated from satellite-derived atmospheric CO_2 concentrations, Geophys. Res. Lett., 44, 1537–1544, https://doi.org/10.1002/2016GL072042, 2017.

Houweling, S., Breon, F.-M., Aben, I., R¨odenbeck, C., Gloor, M., Heimann, M., and Ciais, P.: Inverse modeling of CO_2 sources and sinks using satellite data: a synthetic inter-comparison of measurement techniques and their performance as a function of space and time, Atmos. Chem. Phys., 4, 523–538, https://doi.org/10.5194/acp-4-523-2004, 2004.

Houweling, S., Aben, I., Breon, F.-M., Chevallier, F., Deutscher, N., Engelen, R., Gerbig, C., Griffith, D., Hungershoefer, K., Macatangay, R., Marshall, J., Notholt, J., Peters, W., and Serrar, S.: The importance of transport model uncertainties for the estimation of CO_2 sources and sinks using satellite measurements, Atmos. Chem. Phys., 10, 9981–9992, https://doi.org/10.5194/acp-10-9981-2010, 2010.

Houweling, S., Baker, D., Basu, S., Boesch, H., Butz, A., Cheval- lier, F., Deng, F., Dlugokencky, E. J., Feng, L., Ganshin, A., Hasekamp, O., Jones, D., Maksyutov, S., Marshall, J., Oda, T., O'Dell, C. W., Oshchepkov, S., Palmer, P. I., Peylin, P., Poussi, Z., Reum, F., Takagi, H., Yoshida, Y., and Zhuravlev, R.: An intercomparison of inverse models for estimating sources and sinks of CO_2 using GOSAT measurements, J. Geophys. Res.-Atmos., 120, 5253–5266, https://doi.org/10.1002/2014JD022962, 2015.

Hungershoefer, K., Breon, F.-M., Peylin, P., Chevallier, F., Rayner, P., Klonecki, A., Houweling, S., and Marshall, J.: Evaluation of various observing systems for the global monitoring of CO_2 surface fluxes, Atmos. Chem. Phys., 10, 10503–10520, https://doi.org/10.5194/acp-10-10503-2010, 2010.

Jiang, Z., Jones, D. B. A., Kopacz, M., Liu, J., Henze, D. K., and Heald, C.: Quantifying the impact of model errors on top-down estimates of carbon monoxide emissions using satellite observations, J. Geophys. Res., 116, D15306, https://doi.org/10.1029/2010JD015282, 2011.

Kim, B. Y., Fleming, G. G., Lee, J. J., Waitz, I. A., Clarke, J.-P., Balasubramanian, S., Malwitz, A., Klima, K., Locke, M., Holsclaw, C. A., Maurice, L. Q., Gupta, M. L.: System for assessing Aviation's Global Emissions (SAGE), Part 1: Model description and inventory results, Transportation Research Part D: Transport and Environment, 12(5), 325-346, https://doi.org/10.1016/j.trd.2007.03.007, 2007.

Kim, J., Kim, H. M., Cho, C.-H., Boo, K.-O., Jacobson, A. R., Sasakawa, M., Machida, T., Arshinov, M., and Fedoseev, N.: Impact of Siberian observations on the optimization of surface CO_2 flux, Atmos. Chem. Phys., 17, 2881-2899, https://doi.org/10.5194/acp-17-2881-2017, 2017.

Kivi, R., Heikkinen, P., and Kyro, E.: TCCON data from Sodankyla, Finland, Release GGG2014R0. TCCON data archive, hosted by CaltechDATA, California Institute of Technology, Pasadena, CA, U.S.A. https://doi.org/10.14291/tccon.ggg2014.sodankyla01.R0/1149280, 2017.

Kopacz, M., Jacob, D. J., Henze, D. K., Heald, C. L., Streets, D. G., and Zhang, Q.: A comparison of analytical and adjoint Bayesian inversion methods for constraining Asian sources of CO using satellite (MOPITT) measurements of CO columns, J. Geophys. Res., 114, D04305, https://doi.org/10.1029/2007JD009264, 2009.

Kopacz, M., Jacob, D. J., Fisher, J. A., Logan, J. A., Zhang, L., Megretskaia, I. A, Yantosca, R. M., Singh, K., Henze, D. K., Burrows, J. P., Buchwitz, M., Khlystova, I., McMillan, W. W., Gille, J. C., Edwards, D. P., Eldering, A., Thouret, V., and Nedelec, P.: Global estimates of CO sources with high resolution by adjoint inversion of multiple satellite datasets (MOPITT, AIRS, SCIAMACHY, TES), Atoms. Chem. Phys., 10, 855-876, 2010.

Kuze, A., Suto, H., Nakajima, M., and Hamazaki, T.: Thermal and near infrared sensor for carbon observation Fourier-transform spectrometer on the Greenhouse Gases Observing Satellite for greenhouse gases monitoring. Appl. Opt., 48, 6716, https://doi.org/10.1364 /AO.48.006716, 2009.

Le Quéré, C., Andrew, R. M., Friedlingstein, P., Sitch, S., Pongratz, J., Manning, A. C., Korsbakken, J. I., Peters, G. P., Canadell, J. G., Jackson, R. B., Boden, T. A., Tans, P. P., Andrews, O. D., Arora, V. K., Bakker, D. C. E., Barbero, L., Becker, M., Betts, R. A., Bopp, L., Chevallier, F., Chini, L. P., Ciais, P., Cosca, C. E., Cross, J., Currie, K., Gasser, T., Harris, I., Hauck, J., Haverd, V., Houghton, R. A., Hunt, C. W., Hurtt, G., Ilyina, T., Jain, A. K., Kato, E., Kautz, M., Keeling, R. F., Klein Goldewijk, K., Körtzinger, A., Landschützer, P., Lefèvre, N., Lenton, A., Lienert, S., Lima, I., Lombardozzi, D., Metzl, N., Millero, F., Monteiro, P. M. S., Munro, D. R., Nabel, J. E. M. S., Nakaoka, S.-I., Nojiri, Y., Padin, X. A., Peregon, A., Pfeil, B., Pierrot, D., Poulter, B., Rehder, G., Reimer, J., Rödenbeck, C., Schwinger, J., Séférian, R., Skjelvan, I., Stocker, B. D., Tian, H., Tilbrook, B., Tubiello, F. N., van der Laan-Luijkx, I. T., van der Werf, G. R., van Heuven, S., Viovy, N., Vuichard, N., Walker, A. P., Watson, A. J., Wiltshire, A. J., Zaehle, S., and Zhu, D.: Global Carbon Budget 2017, Earth Syst. Sci. Data, 10, 405-448, https://doi.org/10.5194/essd-10-405-2018, 2018.

Liu, J., Bowman, K. W., Lee, M., Henze, D. K., Bousserez, N., Brix, H., Collatz, G. J., Menemenlis, D., Ott, L., Pawson, S., Jones, D., and Nassar, R.: Carbon monitoring system flux estimation and attribution: impact of ACOS-GOSAT XCO_2 sampling on the inference of terrestrial biospheric sources and sinks, Tellus B, 66, 22486, https://doi.org/10.3402/tellusb.v66.22486, 2014.

658 Liu, J., Bowman, K. W., Schimel, D. S., Parazoo, N. C., Jiang, Z., Lee, M., Bloom, A. A., Wunch, D., Frank-
659 enberg, C., Sun, Y., O'Dell, C. W., Gurney, K. R., Menemenlis, D., Gierach, M., Crisp, D., and Eldering,
660 A.: Contrasting carbon cycle responses of the tropical continents to the 2015–2016 El Niño, Science, 358,
661 eaam5690, https://doi.org/10.1126/science.aam5690, 2017.

662 Maksyutov, S., Takagi, H., Valsala, V. K., Saito, M., Oda, T., Saeki, T., Belikov, D. A., Saito, R., Ito, A., Yo-
663 shida, Y., Morino, I., Uchino, O., Andres, R. J., and Yokota, T.: Regional CO_2 flux estimates for 2009–
664 2010 based on GOSAT and ground- based CO_2 observations, Atmos. Chem. Phys., 13, 9351–9373,
665 https://doi.org/10.5194/acp-13-9351-2013, 2013.

666 Miller, C. E., Crisp, D., DeCola, P. L., Olsen, S. C., Randerson, J. T., Michalak, A. M., Alkhaled, A., Rayner,
667 P., Jacob, D. J., Suntharalingam, P., Jones, D. B. A., Denning, A. S., Nicholls, M. E., Doney, S. C., Paw-
668 son, S., Boesch, H., Connor, B. J., Fung, I. Y., O'Brien, D., Salawitch, R. J., Sander, S. P., Sen, B., Tans,
669 P., Toon, G. C.,Wennberg, P. O.,Wofsy, S. C., Yung, Y. L., and Law, R. M.: Precision requirements for
670 space-based XCO_2 data, J. Geophys. Res., 112, D10314, https://doi.org/10.1029/2006JD007659, 2007.

671 Miller, S. M., Michalak, A. M., Yadav, V., and Tadić, J. M.: Characterizing biospheric carbon balance using
672 CO_2 observations from the OCO-2 satellite, Atmos. Chem. Phys., 18, 6785-6799,
673 https://doi.org/10.5194/acp-18-6785-2018, 2018.

674 Morino, I., Matsuzaki, T., and Shishime, A.: TCCON data from Tsukuba, Ibaraki, Japan, 125HR,
675 Release GGG2014R2. TCCON data archive, hosted by CaltechDATA, California Institute of
676 Technology, Pasadena, CA, U.S.A. http://doi.org/10.14291/tccon.ggg2014.tsukuba02.R2,
677 2017.

678 Nassar, R., Jones, D. B. A., Suntharalingam, P., Chen, J. M., Andres, R. J., Wecht, K. J., Yantosca, R. M., Ku-
679 lawik, S. S., Bowman, K. W., Worden, J. R., Machida, T., and Matsueda, H.: Modeling global atmos-
680 pheric CO_2 with improved emission inventories and CO_2 production from the oxidation of other carbon
681 species, Geosci. Model Dev., 3, 689–716, https://doi.org/10.5194/gmd-3-689-2010, 2010.

682 Nassar, R., Hill, T. G., McLinden, C. A., Wunch, D., Jones, D. B. A., and Crisp, D.: Quantifying CO_2 emis-
683 sions From Individual Power Plants from Space, Geophys. Res. Lett., 44, 10045– 10053,
684 https://doi.org/10.1002/2017GL074702, 2017.

685 Notholt, J., Petri, C., Warneke, T., Deutscher, N., Buschmann, M., Weinzierl, C., Macatangay,
686 R., and Grupe, P.: TCCON data from Bremen, Germany, Release GGG2014R0. TCCON data
687 archive, hosted by CaltechDATA, California Institute of Technology, Pasadena, CA, U.S.A.
688 https://doi.org/10.14291/tccon.ggg2014.bremen01.R0/1149275, 2017a.

689 Notholt, J., Schrems, O., Warneke, T., Deutscher, N., Weinzierl, C., Palm, M., Buschmann, M.,
690 and AWI-PEV Station Engineers: TCCON data from Ny Alesund, Spitzbergen, Norway, Re-
691 lease GGG2014R0. TCCON data archive, hosted by CaltechDATA, California Institute of
692 Technology, Pasadena, CA, U.S.A. https://doi.org/10.14291/tccon.ggg2014.nyale-
693 sund01.R0/1149278, 2017b.

694 O'Dell, C., Connor, B., Bösch, H., O'Brien, D., Frankenberg, C., Castano, R., Christi, M., Eldering, D.,
695 Fisher, B., Gunson, M., McDuffie, J., Miller, C. E., Natraj, V., Oyafuso, F., Polonsky, I., Smyth, M., Tay-
696 lor, T., Toon, G., Wennberg, P., and Wunch, D.: The ACOS CO_2 retrieval algorithm – Part 1: Description
697 and validation against synthetic observations, Atmos. Meas. Tech., 5, 99-121, https://doi.org/10.5194/amt-
698 5-99-2012, 2012.

699 Park, B. C. and Prather, M. J.: CO_2 source inversions using satellite observations of the upper troposphere,
700 Geophys. Res. Lett., 28, 4571–4574, https://doi.org/10.1029/2001GL013604, 2001.

701 Parrington, M., Palmer, P. I., Henze, D. K., Tarasick, D. W., Hyer, E. J., Owen, R. C., Clerbaux, C., Bowman,
702 K. W., Deeter, M. N., Barratt, E. M., Coheur, P.-F., Hurtmans, D., George, M., and Worden, J. R.: The in-
703 fluence of boreal biomass burning emissions on the distribution of tropospheric ozone over North Amer-
704 ica and the North Atlantic during 2010, Atmos. Chem. Phys., 12, 2077-2098, 2012.

705 Patra, P. K., Crisp, D., Kaiser, J. W., Wunch, D., Saeki, T., Ichii, K., Sekiya, T., Wennberg, P. O., Feist, D. G.,
706 Pollard, D. F., Griffith, D. W. T., Velazco, V. A., De Maziere, M., Sha, M. K., Roehl, C., Chatterjee, A.,

and Ishijima, K.: The Orbiting Carbon Observa- tory (OCO-2) tracks 2–3 peta-gram increase in carbon release to the atmosphere during the 2014–2016 El Niño, Sci. Rep.-UK, 7, 13567, https://doi.org/10.1038/s41598-017-13459-0, 2017.

Peters, W., Jacobson, A. R., Sweeney, C., Andrews, A. E., Conway, T. J., Masarie, K., Miller, J. B., Bruhwiler, L. M. P., P´etron, G., Hirsch, A. I.,Worthy, D. E. J.,Werf, G. R. V. D., Randerson, J. T., Wennberg, P. O., Krol, M. C., and Tans, P. P.: An atmospheric perspective on North American carbon dioxide exchange: CarbonTracker, P. Natl. Acad. Sci., 104, 18925–18930, 2007..

Peylin, P., Law, R. M., Gurney, K. R., Chevallier, F., Jacobson, A. R., Maki, T., Niwa, Y., Patra, P. K., Peters, W., Rayner, P. J., Rödenbeck, C., van der Laan-Luijkx, I. T., and Zhang, X.: Global atmospheric carbon budget: results from an ensemble of atmospheric CO_2 inversions, Biogeosciences, 10, 6699–6720, https://doi.org/10.5194/bg-10-6699-2013, 2013.

Potter, C. S., Randerson, J. T., Field, C. B., Matson, P. A., Vitousek, P. M., Mooney, H. A., and Klooster, S. A.: Terrestrial ecosystem production: A process model based on global satellite and surface data, Global Biogeochem. Cycles, 7(4), 811–841, https://doi.org/10.1029/93GB02725, 1993.

Rayner, P. J. and O'Brien, D. M.: The utility of remotely sensed CO_2 concentration data in surface source inversions, Geophys. Res. Lett., 28, 175–178, https://doi.org/10.1029/2000GL011912, 2001.

Reuter, M., Buchwitz, M., Hilker, M., Heymann, J., Schneising, O., Pillai, D., Bovensmann, H., Burrows, J. P., Bösch, H., Parker, R., Butz, A., Hasekamp, O., O'Dell, C. W., Yoshida, Y., Gerbig, C., Nehrkorn, T., Deutscher, N. M., Warneke, T., Notholt, J., Hase, F., Kivi, R., Sussmann, R., Machida, T., Matsueda, H., and Sawa, Y.: Satellite-inferred European carbon sink larger than expected, Atmos. Chem. Phys., 14, 13739-13753, https://doi.org/10.5194/acp-14-13739-2014, 2014.

Reuter, M., Buchwitz, M., Hilker, M., Heymann, J., Bovensmann, H., Burrows, J. P., Houweling, S., Liu, Y. Y., Nassar, R., Chevallier, F., Ciais, P., Marshall, J., and Reichstein, M.: How Much CO_2 Is Taken Up by the European Terrestrial Biosphere?. Bull. Amer. Meteor. Soc., 98, 665–671, https://doi.org/10.1175/BAMS-D-15-00310.1, 2017.

Rienecker, M. M., Suarez, M. J., Todling, R., Bacmeister, J., Takacs, L. and co-authors: The GEOS-5 Data Assimilation System-Documentation of versions 5.0.1 and 5.1.0, and 5.2.0 NASA Tech. Rep. Series on Global Modeling and Data Assimilation, NASA/TM-2008-104606, Vol. 27, 92 pp, 2008.

Rodgers, C. D.: Inverse Methods for Atmospheric Sounding: Theory and Practice, World Scientific Publishing Co Inc, Singapore, chapter 2, 2000.

Saeki, T., Maksyutov, S., Saito, M., Valsala, V., Oda, T., An- dres, R. J., Belikov, D., Tans, P., Dlugokencky, E., Yoshida, Y., Morino, I., Uchino, O., and Yokota, T.: Inverse modeling of CO_2 fluxes using GOSAT data and multi-year ground-based obser- vations, SOLA, 9, 45–50, https://doi.org/10.2151/sola.2013-011, 2013.

Sherlock, V., Connor, B., Robinson, J., Shiona, H., Smale, D., and Pollard, D.: TCCON data from Lauder, New Zealand, 125HR, Release GGG2014R0. TCCON data archive, hosted by CaltechDATA, California Institute of Technology, Pasadena, CA, U.S.A. https://doi.org/10.14291/tccon.ggg2014.lauder02.R0/1149298, 2017.

Singh, K., Jardak, M., Sandu, A., Bowman, K., Lee, M., and Jones, D.: Construction of non-diagonal background error covariance matrices for global chemical data assimilation, Geosci. Model Dev., 4, 299-316, https://doi.org/10.5194/gmd-4-299-2011, 2011.

Suntharalingam, P., Jacob, D. J., Palmer, P. I., Logan, J. A., Yantosca, R. M. and co-authors: Improved quantification of Chinese carbon fluxes using CO_2/CO correlations in Asian outflow. J. Geophys. Res. 109, D18S18, https://doi.org/10.1029/2003JD004362, 2004.

Sussmann, R., and Rettinger, M.: TCCON data from Garmisch, Germany, Release GGG2014R2. TCCON data archive, hosted by CaltechDATA, California Institute of Technology, Pasadena, CA, U.S.A. https://doi.org/10.14291/tccon.ggg2014.garmisch01.R2, 2017.

Takagi, H., Saeki, T., Oda, T., Saito, M., Valsala, V., Belikov, D., Saito, R., Yoshida, Y., Morino, I., Uchino,

O., Andres, R. J., Yokota, T., and Maksyutov, S.: On the benefit of GOSAT observations to the estimation of regional CO_2 fluxes, SOLA, 7, 161–164, https://doi.org/10.2151/sola.2011-041, 2011.

Tarantola, A.: Inverse Problem Theory and Methods for Model Parameter Estimation, Soc. Industr. App.l Math., Philadelphia, PA, USA, 2004.

van der Werf, G. R., Randerson, J. T., Giglio, L., Collatz, G. J., Mu, M., Kasibhatla, P. S., Morton, D. C., DeFries, R. S., Jin, Y., and van Leeuwen, T. T.: Global fire emissions and the contribution of deforestation, savanna, forest, agricultural, and peat fires (1997–2009), Atmos. Chem. Phys., 10, 11707–11735, https://doi.org/10.5194/acp-10-11707-2010, 2010.

Wang, X., Guo, Z., Huang, Y. P., Fan, H. J., and Li, W. B.: A cloud detection scheme for the Chinese carbon dioxide observation satellite (TANSAT). Adv. Atmos. Sci., 34(1), 16–25, https://doi.org/10.1007/s00376-016-6033-y, 2017.

Warneke, T., Messerschmidt, J., Notholt, J., Weinzierl, C., Deutscher, N., Petri, C., Grupe, P., Vuillemin, C., Truong, F., Schmidt, M., Ramonet, M., and Parmentier, E.: TCCON data from Orleans, France, Release GGG2014R0. TCCON data archive, hosted by CaltechDATA, California Institute of Technology, Pasadena, CA, U.S.A. https://doi.org/10.14291/tccon.ggg2014.orleans01.R0/1149276, 2017.

Wennberg, P. O., Roehl, C., Wunch, D., Toon, G. C., Blavier, J.-F., Washenfelder, R., Keppel-Aleks, G., Allen, N., and Ayers, J.: TCCON data from Park Falls, Wisconsin, USA, Release GGG2014R1. TCCON data archive, hosted by CaltechDATA, California Institute of Technology, Pasadena, CA, U.S.A. http://doi.org/10.14291/tccon.ggg2014.parkfalls01.R1, 2017.

Wennberg, P. O., Wunch, D., Roehl, C., Blavier, J.-F., Toon, G. C., Allen, N., Dowell, P., Teske, K., Martin, C., and Martin, J.: TCCON data from Lamont, Oklahoma, USA, Release GGG2014R1. TCCON data archive, hosted by CaltechDATA, California Institute of Technology, Pasadena, CA, U.S.A. https://doi.org/10.14291/tccon.ggg2014.lamont01.R1/1255070, 2017. Wilkerson, J. T., Jacobson, M. Z., Malwitz, A., Balasubramanian, S., Wayson, R., Fleming, G., Naiman, A. D., and Lele, S. K.: Analysis of emission data from global commercial aviation: 2004 and 2006, Atmos. Chem. Phys., 10, 6391-6408, https://doi.org/10.5194/acp-10-6391-2010, 2010.

Wunch, D., Wennberg, P. O., Toon, G. C., Connor, B. J., Fisher, B., Osterman, G. B., Frankenberg, C., Mandrake, L., O'Dell, C., Ahonen, P., Biraud, S. C., Castano, R., Cressie, N., Crisp, D., Deutscher, N. M., Eldering, A., Fisher, M. L., Griffith, D. W. T., Gunson, M., Heikkinen, P., Keppel-Aleks, G., Kyrö, E., Lindenmaier, R., Macatangay, R., Mendonca, J., Messer- schmidt, J., Miller, C. E., Morino, I., Notholt, J., Oyafuso, F. A., Rettinger, M., Robinson, J., Roehl, C. M., Salawitch, R. J., Sherlock, V., Strong, K., Sussmann, R., Tanaka, T., Thomp- son, D. R., Uchino, O., Warneke, T., and Wofsy, S. C.: A method for evaluating bias in global measurements of CO_2 total columns from space, Atmos. Chem. Phys., 11, 12317–12337, https://doi.org/10.5194/acp-11-12317-2011, 2011.

Wunch, D., Wennberg, P. O., Osterman, G., Fisher, B., Naylor, B., Roehl, C. M., O'Dell, C., Mandrake, L., Viatte, C., Kiel, M., Griffith, D. W. T., Deutscher, N. M., Velazco, V. A., Notholt, J., Warneke, T., Petri, C., De Maziere, M., Sha, M. K., Sussmann, R., Rettinger, M., Pollard, D., Robinson, J., Morino, I., Uchino, O., Hase, F., Blumenstock, T., Feist, D. G., Arnold, S. G., Strong, K., Mendonca, J., Kivi, R., Heikkinen, P., Iraci, L., Podolske, J., Hillyard, P. W., Kawakami, S., Dubey, M. K., Parker, H. A., Sepulveda, E., García, O. E., Te, Y., Jeseck, P., Gunson, M. R., Crisp, D., and Eldering, A.: Comparisons of the Orbiting Carbon Observatory-2 (OCO-2) XCO_2 measurements with TCCON, At- mos. Meas. Tech., 10, 2209–2238, https://doi.org/10.5194/amt- 10-2209-2017, 2017.

Yang, D. X., Liu, Y., Cai, Z. N., Chen, X., Yao, L., and Lu, D. R.: First global carbon dioxide maps produced from TanSat measurements. Adv. Atmos. Sci., 35(6), 621–623, https://doi.org/10.1007/s00376-018-7312-6, 2018.

Zhu, C., Byrd, R. H., Lu, P. and Nocedal, J.: L-BFGS-B: algorithm 778: L-BFGS-B, FORTRAN routines for large scale bound constrained optimization. ACM Trans. Math. Softw. 23(4), 550_560. https://doi.org/10.1145/279232.279236, 1997.